IAI Journals.ASM.org

Helicobacter pylori Requires TlpD-Driven Chemotaxis To Proliferate in the Antrum

Annah S. Rolig,[a] James Shanks,[a] J. Elliot Carter,[b] and Karen M. Ottemann[c]

Department of Molecular, Cellular, and Developmental Biology, University of California, Santa Cruz, Santa Cruz, California, USA[a]; Department of Pathology, University of South Alabama College of Medicine, Mobile, Alabama, USA[b]; and Department of Microbiology and Environmental Toxicology, University of California, Santa Cruz, Santa Cruz, California, USA[c]

Different disease outcomes of *Helicobacter pylori* infection correlate with distinct inflammation patterns. These different inflammatory distributions may be initiated by differences in bacterial localization. One *H. pylori* property known to affect murine stomach localization is chemotaxis, the ability to move in response to chemical cues. In this report, we used nonchemotactic mutants (Che$^-$) to analyze whether chemotaxis is required for initial colonization of particular stomach regions or for subsequent growth therein. We found that *H. pylori* behaves differently in the corpus, antrum, and corpus-antrum transition zone subregions of the stomach. This outcome suggests that these regions contain unique chemotactic signals. In the corpus, *H. pylori* utilizes chemotaxis for initial localization but not for subsequent growth. In contrast, in the antrum and the corpus-antrum transition zone, chemotaxis does not help initial colonization but does promote subsequent proliferation. To determine which chemoreceptor is responsible for the corpus-antrum phenotypes, we infected mice with strains lacking each chemoreceptor. Strains lacking TlpA, TlpB, or TlpC displayed only modest deviations from the wild-type phenotype, while strains lacking TlpD resembled the Che$^-$ mutant in their antral colonization defect and fared even worse than the Che$^-$ mutant in the corpus. Additional analysis showed that inflammation is worse in the antrum than in the corpus in both wild-type and Che$^-$ mutant infections. These results suggest that chemotaxis, specifically, that controlled by TlpD, is necessary for *H. pylori* to survive or grow in the environment of increased inflammation in the antrum.

The gastric pathogen *Helicobacter pylori* chronically infects the stomachs of 50% of the world's population. Infection with *H. pylori* triggers gastric inflammation, also known as gastritis, which can lead to a wide range of disease outcomes, such as mild gastritis, gastric and peptic ulcers, gastric adenocarcinoma, and mucosa-associated lymphoid tissue (MALT) lymphoma (38). *H. pylori*-induced gastritis occurs most frequently in the antrum (A) (3, 26, 49), one of four distinct regions in the human stomach (19, 28). Each region is defined by the cell types that exist in the gastric glands. The two largest stomach regions are the antrum and the corpus (C), and a third region, the corpus-antrum (C-A) transition zone, separates them. Multiple lines of evidence suggest that *H. pylori*-triggered inflammation in each of these regions results in distinct disease outcomes. For example, gastritis that affects predominantly the antrum correlates with *H. pylori*-triggered duodenal ulcers (3, 56), a disease state that does not develop to gastric cancer (3, 45, 49). Gastritis that predominantly affects the corpus, in contrast, increases the risk of gastric ulcers and intestinal gastric cancer (3, 49), while gastritis throughout the stomach, so-called pangastritis, increases the risk for diffuse gastric cancer (49). These observations demonstrate that specific *H. pylori* diseases correlate with inflammation in specific stomach regions. The basis for these different patterns of inflammation is unclear, but one possible reason for the differential locations of diseased tissue is that different *H. pylori* strains preferentially colonize either the antrum or the corpus and in turn trigger elevated inflammation in that region. Thus, the localization of *H. pylori* within the stomach may be important for driving disease development.

Studies have shown that different *H. pylori* strains achieve higher bacterial colonization numbers in either the corpus or the antrum (1, 27, 33). For example, strain X47 has a strong preference for the corpus, and strain SS1 has an antral preference or colonizes the antrum and corpus equally, depending on the study (1, 27, 47). Three *H. pylori* characteristics have been found that influence stomach localization: (i) the presence of a cytotoxin-associated pathogenicity island, or *cag*-PAI (40); (ii) the presence of the ferric uptake regulator (Fur) (33), which is necessary for *H. pylori* adaptation to various conditions, including iron limitation (50), acid stress, and oxidative stress (6, 14); and (iii) the bacterial ability to be chemotactic, or to move in response to chemical cues (47).

Bacterial chemotaxis has been extensively studied in *Escherichia coli* and thus serves as a model for other bacteria (34, 52). Chemotactic responses initiate when chemoreceptors detect environmental cues and transmit information to CheA, a histidine kinase, via CheW, the coupling protein. In the absence of chemotaxis attractants, the ligand-free chemoreceptors activate the CheA histidine kinase, which in turn phosphorylates the response regulator CheY. Phosphorylated CheY (CheY-P) interacts with the flagellar motor to cause clockwise flagellar rotation and random bacterial movement. Conversely, when the chemoreceptors bind a chemoattractant ligand, the CheA histidine kinase is inactivated and CheY-P populations are reduced and replaced with nonphosphorylated CheY. Nonphosphorylated CheY does not in-

Received 19 April 2012 Returned for modification 13 May 2012
Accepted 10 July 2012
Published ahead of print 16 July 2012
Editor: A. Camilli
Address correspondence to Karen M. Ottemann, ottemann@ucsc.edu.

doi:10.1128/IAI.00407-12

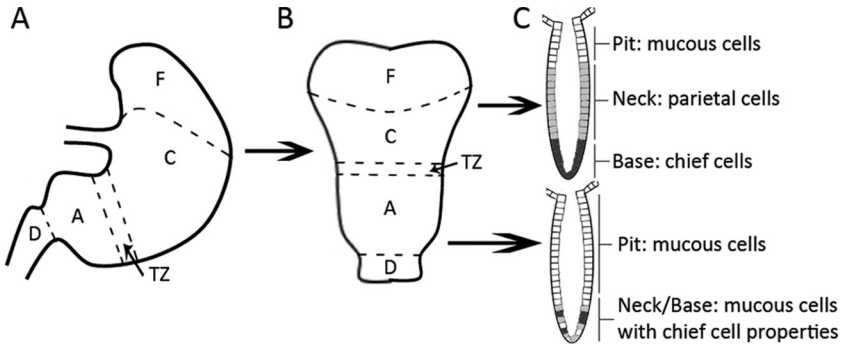

FIG 1 A diagram of the different physiological regions of the mouse stomach (28). (A) Side view of the stomach regions. (B) The stomach is opened up along the lesser curvature and divided down the middle along the longitudinal axis. (C) Representation of the different cell types found in the glands of the antrum and the corpus. F, forestomach; C, corpus; TZ, C-A transition zone; A, antrum; D, duodenum.

teract with the flagellar motor, which in turn rotates in the default counterclockwise direction, and the bacteria swim in a straight line.

The chemotaxis system of *H. pylori* is similar to that of *E. coli* (29). *H. pylori* has the core signaling complex proteins CheW, CheA, and CheY, and disruption of any of these core proteins renders *H. pylori* nonchemotactic (5, 15, 37). *H. pylori* has three membrane-bound chemoreceptors, TlpA, TlpB, and TlpC, and one cytoplasmic chemoreceptor, TlpD (29). TlpA has been shown to sense arginine and bicarbonate (7), and TlpB has been shown to sense pH (10, 20) and autoinducer-2 (AI-2), the quorum-sensing molecule (39). TlpD is involved in energy taxis (44), and the ligands for TlpC are unknown.

Individual *H. pylori* strain SS1 chemoreceptor mutants colonize the mouse stomach to wild-type levels (2, 28) but fare less well in coinfections with the wild type. Specifically, mutants lacking TlpA or TlpC are outcompeted 25-to-50-fold by the wild type (2), while those lacking TlpB are not (31, 54). In comparison, nonchemotactic *H. pylori* SS1 mutants (Che^-) that lack core-signaling components such as CheW, CheA, or CheY are outcompeted more than 1,000-fold. These Che^- mutants additionally have colonization defects during the first 2 weeks of infection when they are the sole infecting strain (47). After 2 weeks, Che^- mutants achieve wild-type colonization levels; however, they have a different distribution throughout the stomach. Unlike the wild type, Che^- mutants have a striking inability to colonize the antrum, while they occupy the corpus at only modestly decreased levels compared to the wild type (47). Thus far, it is unknown why antral localization requires chemotaxis. Chemotaxis may be necessary to locate the antrum or to maintain colonization there, and one of the four chemoreceptors may be specifically responsible for the localization defects.

Since *H. pylori* infections are associated with antral gastritis (3, 26, 49), we found it interesting that bacterial chemotaxis both drives antral localization (47) and increases the inflammatory response to *H. pylori* (31, 41, 54). Therefore, we undertook this study to determine if chemotaxis is necessary for *H. pylori* to locate the antrum or to remain there after initial colonization and to determine which chemoreceptor is responsible for this localization phenotype.

MATERIALS AND METHODS

***H. pylori* strains and growth conditions.** *H. pylori* strain SS1 (27) and its isogenic mutants were used for all studies. SS1 was a gift of Jani O'Rourke (University of New South Wales) and was subjected to minimal laboratory passage before our experiments. SS1 Δ*cheY*::*cat*, Δ*tlpA*::*cat*, Δ*tlpB*::*cat*, Δ*tlpC*::*cat*, and Δ*tlpD*::*cat* were described previously (2, 31, 47, 54), and all have most of the target gene replaced with the *Campylobacter cat* gene. *H. pylori* was cultured on Columbia blood agar (Remel) with 5% difibrinated horse blood (Hemostat Laboratories, Davis, CA), 50 μg/ml cycloheximide, 10 μg/ml vancomycin, 5 μg/ml cefsulodin, 2.5 U/ml polymyxin B, and 0.2% β-cyclodextrin. Mouse stomach samples were plated on the same medium plus 5 μg/ml trimethoprim, 8 μg/ml amphotericin B, 10 μg/ml nalidixic acid, and 200 μg/ml bacitracin. To prepare *H. pylori* for mouse infection, we grew the bacteria with shaking in brucella broth (Becton, Dickinson and Company) with 10% fetal bovine serum (FBS; Gibco) (BB10). Cultures were incubated at 37°C with 7 to 10% O_2, 10% CO_2, and 80 to 83% N_2, with chloramphenicol at 13 μg/ml to select for the various mutants as needed. For mouse infection, we inoculated animals orally intragastrically via a feeding needle (20 gauge by 1.5 in.) with a 500-μl inoculum containing ~1×10^7 CFU/ml brucella broth-grown *H. pylori*.

Animal infections. The University of California (U.C.) Santa Cruz Institutional Animal Care and Use Committee approved all animal protocols and experiments. Female C57Bl6/N mice (*Helicobacter*-free) (Taconic Laboratories, Germantown, NY) and female and male FVB/N mice (*Helicobacter*-free) (Charles River Laboratories) were housed at the animal facility of the U.C. Santa Cruz. Mice were between 6 and 8 weeks old at the time of *H. pylori* infection, and age-matched uninfected mice were included in all experiments. After the infection period, the animals were sacrificed via CO_2 narcosis, and the stomach was dissected, opened along the lesser curvature, and divided into four parts—the corpus, the transition zone, the antrum, and the upper duodenum (Fig. 1). The nonglandular forestomach was identified as a yellow, thin tissue structure; it was removed from the stomach and not included in experimental analysis. The corpus is a brownish, thick-walled section of tissue, and the antrum is a paler, pinkish, thinner-walled section. The transition zone is an ~1.0-mm-wide region demarcating these two sections. These regions were identified as described by Lee et al. (28). The tissue pieces were homogenized using a Bullet Blender (Next Advance) with 1.0-mm-diameter zirconium silicate beads and plated to determine the number of *H. pylori* CFU/gram of stomach.

Histology and pathology. After dissection, half of the stomach was placed in a histology cassette with a sponge (Fisher) and preserved in buffered formalin (Fisher). The tissue was embedded in paraffin, sectioned (5-μm slices), stained with hematoxylin and eosin, and evaluated in a blinded manner by a pathologist (J. E. Carter). Each stomach slice received a separate grade for each region of the stomach. Each slide was evaluated twice. Lymphocytic infiltration was scored as outlined by Eaton et al. (11), using scoring as follows: 0, no infiltrate; 1,

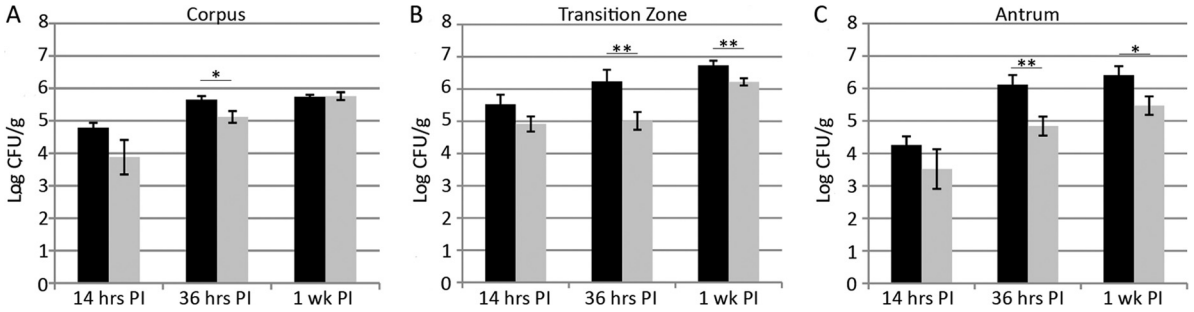

FIG 2 Chemotaxis is required for antral colonization at time points after 14 h postinoculation (PI). Female FVB/N mice were infected with the SS1 wild type (black bars) or the isogenic Che$^-$ mutant (gray bars) for 14 h, 36 h, or 1 week. At each time point, stomachs were removed, and divided into the corpus (A), the C-A transition zone (B), and the antrum (C) and plated to determine *H. pylori* colonies. Error bars indicate standard error of the mean. $n = 8$ or 9 for 14 and 36 h, derived from two independent infections. $n = 7$ for 1 week, derived from one independent infection. *, $P < 0.05$; **, $P < 0.01$ (Student's *t* test). Data were also used for the doubling-time calculations in Table 1 and shown in Fig. 3.

mild, multifocal infiltration; 2, mild, widespread infiltration; 3, mild, widespread, and moderate multifocal infiltration; 4, moderate, widespread infiltration; and 5, moderate, widespread, and severe multifocal infiltration. Neutrophils were noted as either present or absent (data not shown). Gastric atrophy was assessed using the method of Rugge et al. (42) but was not present in any sample.

RESULTS

Chemotaxis is necessary for *H. pylori* to remain in the antrum after infection has established. Terry et al. reported previously that Che$^-$ *H. pylori* bacteria are barely found in the murine antrum at 2 weeks postinoculation compared to wild-type *H. pylori* (47). This finding is consistent with chemotaxis either directing the bacteria to initially locate the antrum or allowing the bacteria to remain in the antrum after infection has been established. To determine at what point chemotaxis was needed in infection, we examined the numbers of wild-type and Che$^-$ *H. pylori* bacteria in the corpus, transition zone, and antrum at early time points (14 h) compared to later time points postinoculation. For our first time point, we wanted only to enumerate stably infecting bacteria, so we chose 14 h postinoculation, a time well after the 3 h required for the mouse stomach to empty from one feeding (46). At 14 h postinoculation, Che$^-$ bacteria did not have a substantial initial colonization defect in either the transition zone or the antrum, as indicated by numbers that did not differ significantly from those of the wild type (Fig. 2B and C). Interestingly, by 36 h postinoculation in these regions, the Che$^-$ *H. pylori* population had undergone only a modest increase in numbers compared to the substantial increase in wild-type numbers, and thus Che$^-$ colonization levels were significantly lower in the transition zone and the antrum. We observed that this phenotype remained at 1 week postinoculation (Fig. 2B and C), similar to what had been observed previously at 2 weeks (47). These results suggest that chemotaxis does not promote the initial antrum or transition zone seeding but is very important during the increase in *H. pylori* numbers that occurs from 14 h to 1 week postinoculation in these regions.

In the corpus, Che$^-$ *H. pylori* colonization levels were somewhat lower at 14 h and remained so at 36 h, suggesting that chemotaxis plays a minor role in the initial seeding of this stomach region. Between 36 h and 1 week, numbers of both wild-type and Che$^-$ *H. pylori* bacteria increased such that they were nearly equal at 1 week postinoculation (Fig. 2A). Thus, it seems that chemotaxis is not needed for bacterial multiplication in the corpus.

We also examined the upper duodenum to identify if bacteria were washed out of the stomach into the duodenum. However, *H. pylori* colonies rarely grew from the duodenal samples, suggesting that the *H. pylori* bacteria were dead, unculturable, or present in the duodenum at numbers below our limit of detection (~200 CFU per gram) (data not shown). We are therefore not able to estimate the contribution of bacterial loss due to flow out of the stomach.

To estimate the doubling time of *H. pylori* colonies early in infection, when the bacterial numbers are increasing, we reasoned that we could use the equation for unrestricted growth. Early in infection, bacterial numbers are increasing due to multiplication but there is also presumably an unknown rate of removal of bacterial cells due to death and flow out of the stomach. Later in infection, in contrast, bacterial population growth rates are hypothesized to be similar to growth rates in a continuous-flow or chemostat culture although more complicated due to nonuniform nutrient distributions (16–18, 30). The chemotaxis mutants used here do not have *in vitro* growth defects, as measured in BB10 media for the Che$^-$, the Δ*tlpA*, and the Δ*tlpC* mutants (2) and Δ*tlpD* mutants (S. M. Williams and K. M. Ottemann, personal communication). The Δ*tlpB* mutant behavior has not been directly measured, but it has no defect in an assay that depends on growth, the soft agar migration assay, suggesting that it does not have a growth defect (31). We found that the total population of wild-type *H. pylori* doubled approximately every 6.5 h in the corpus and 8 h in the transition zone. In the antrum, in contrast, wild-type *H. pylori* did considerably better, with the population doubling every 3 h (Fig. 3A; Table 1). Similar to that of the wild type, the population of the Che$^-$ mutant doubled approximately every 5.5 h in the corpus. However, in the antrum, the Che$^-$ strain population doubled approximately every 5 h, or at a rate nearly two times lower than that seen with the wild type in this region. Additionally, the Che$^-$ mutant population did not double in the transition zone over this time period (Fig. 3A; Table 1). These data further indicate that chemotaxis promotes growth or prevents *H. pylori* from washing out of the transition zone and antrum.

Competition with wild-type *H. pylori* exacerbates the Che$^-$ *H. pylori* survival defect in the antrum. We also determined how chemotaxis aids stomach region colonization under conditions where this process is more important—the competition infection—at the two earliest time points. For these experiments, we

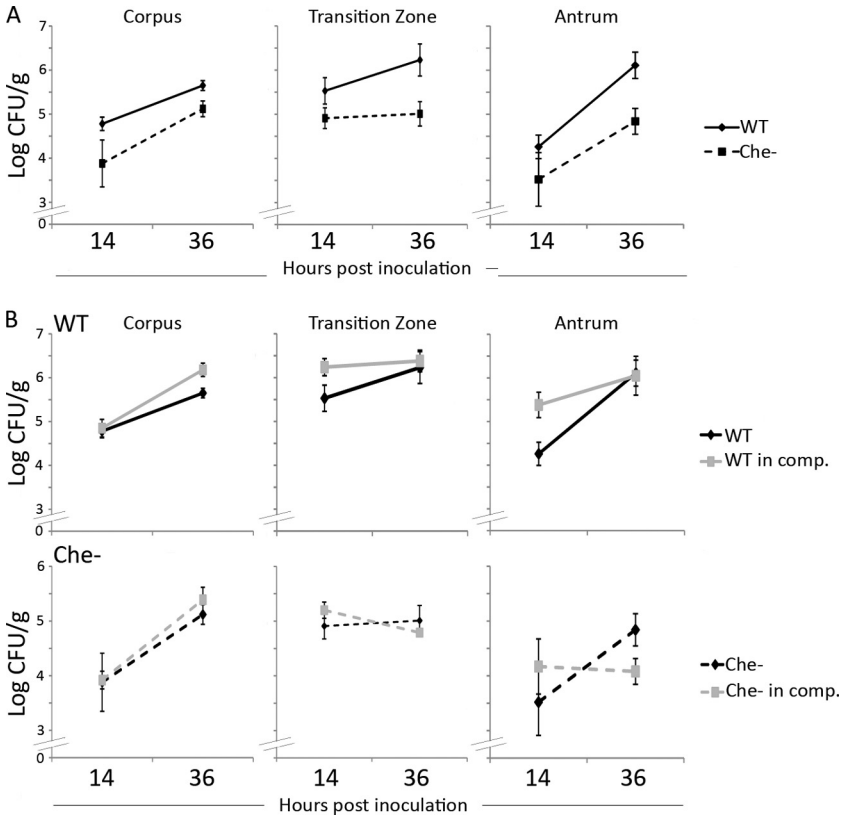

FIG 3 Chemotaxis allows *H. pylori* to grow more quickly in the antrum and provides an advantage in a competition infection. (A) Female FVB/N mice were infected with the SS1 wild type (solid line) or the isogenic Che$^-$ mutant (dotted line) for 14 or 36 h. At each time point, stomachs were removed and divided into the corpus, the C-A transition zone, and the antrum and plated to determine the number of *H. pylori*. $n = 8$ or 9 for the wild type and the Che$^-$ mutant for all time points, derived from two independent infections. Data are also shown in Table 1 and Fig. 2. (B) Competition experiments were carried out by infecting female FVB/N mice with a 1:1 ratio of the wild type and the Che$^-$ mutant for 14 or 36 h. At each time point, stomachs were removed, divided, and plated as described for panel A. Black lines represent each strain in single infection, as described for panel A; gray lines indicate the strains in competition. $n = 5$ for the wild type and the Che$^-$ mutant for all time points, derived from one experiment. Error bars represent standard error of the mean.

infected mice with a mixture of equal amounts of the wild type and the Che$^-$ mutant and assessed numbers of each strain at 14 and 36 h postinoculation as described above. Generally speaking, the numbers of both the wild type and the Che$^-$ mutant were not affected by the presence of the other strain in the corpus and transition zone at 14 or 36 h (Fig. 3B). One possibility is that the total bacterial numbers of both strains were below the threshold at which competition has an effect or, alternatively, that conditions that result in a competitive defect do not exist at those early infection times. The antrum represented a different situation. In this region, numbers of the Che$^-$ mutant did not increase (Fig. 3B). These results show that chemotaxis greatly facilitates bacterial survival or growth in this region, particularly when the wild type is included (Fig. 3B; Table 1).

TABLE 1 Doubling times for *H. pylori* SS1 or its isogenic Che$^-$ (ΔCheY) mutant early after infection[a]

Infection category and strain	Doubling time (h)		
	Corpus	Transition zone	Antrum
Single			
WT	6.46	7.87	3.00
ΔCheY	5.47	57.29	5.20
Competition			
WT	5.28	49.49	10.55
ΔCheY	4.63	No growth	No growth

[a] Doubling time = $(22\ \text{h})/[(\log \text{CFU/gram}^{36\ \text{h}} - \log \text{CFU/gram}^{14\ \text{h}})/\log_2]$. Data are also shown in Fig. 3A.

Enhanced inflammatory responses may contribute to Che$^-$ antral localization defects. Several studies have reported that the majority of gastritis cases are antral dominant in humans (3, 26, 49). Since chemotaxis is necessary for *H. pylori* to remain in the antrum after infection has been established, we speculated that antral immune responses make this localization unfavorable for Che$^-$ *H. pylori*. Reports on the location of gastritis in mice suggest that there is increased inflammation in the corpus-antrum (C-A) transition zone and the antrum at 6 months postinoculation (27), and so we sought to examine if inflammation specifically in the antrum correlates with reduced Che$^-$ colonization. Inflammation is not detectable until after several months of *H. pylori* infection (12), so we examined inflammation and colonization levels in each physiologic region of stomachs from mice infected with wild-type or Che$^-$ *H. pylori* for 3 or 6 months. At these time points, we found that wild-type *H. pylori* induced more inflammation than Che$^-$ overall (Fig. 4B), as reported previously (54). Inflammation in the antrum was higher for both infection types compared to the

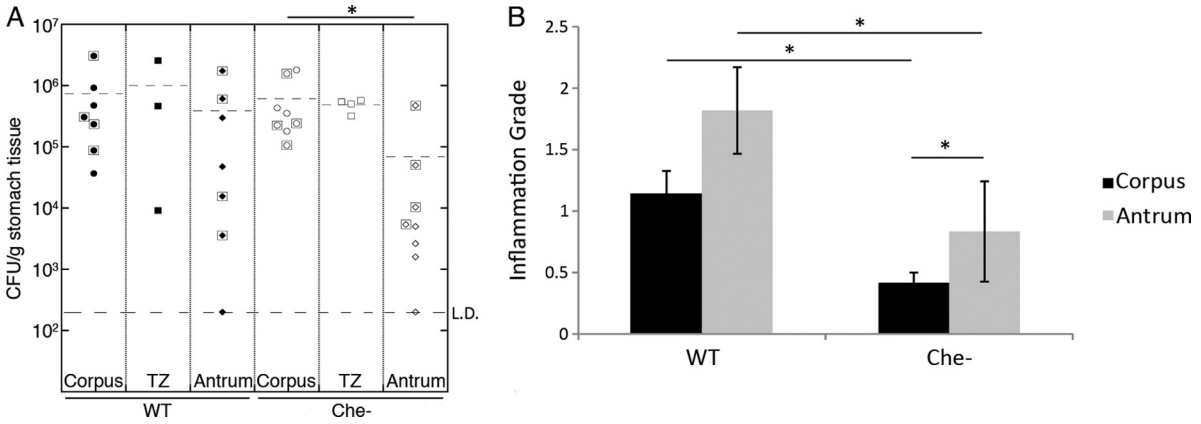

FIG 4 The antrum harbors lower *H. pylori* colonization than other regions and more severe inflammation. (A) *H. pylori* colonization levels as CFU/gram of stomach from female C57BL/6N mice infected for 3 months (symbols surrounded by boxes) or 6 months (symbols without boxes) with *H. pylori* strain SS1 or its isogenic Che$^-$ mutant. $n = 7$ for the wild type, $n = 8$ for the Che$^-$ mutant. (B) Gastric inflammation tissue from mice infected for 6 months was analyzed by a pathologist and graded for inflammation. Error bars indicate standard error of the mean. Data derived from the same 6-month-infected mice as presented in panel A. L.D. = limit of detection. $n = 5$ for the wild type and the Che$^-$ mutant. *, $P < 0.05$ (Student's *t* test).

corpus (Fig. 4B). Additionally, we noted that Che$^-$ strains continued to struggle to colonize the antrum (Fig. 4A). Thus, it appears that the antrum had significantly more inflammation than the corpus and was significantly more challenging for Che$^-$ *H. pylori* to colonize.

The chemoreceptor TlpD is required for growth and/or survival in the antrum. To help distinguish the signals required for colonization of the corpus versus the antrum, we next investigated whether individual chemoreceptor mutants had any distinct antrum or corpus colonization defects. To this end, we infected mice with SS1 Δ*tlpA*::*cat*, SS1 Δ*tlpB*::*cat*, SS1 Δ*tlpC*::*cat*, or SS1 Δ*tlpD*::*cat* and examined the colonization levels of each mutant 2 weeks postinoculation in the corpus and the antrum. As observed previously at this time point (47), the Che$^-$ mutant colonization levels in the antrum were significantly below that of the wild type (Fig. 5A). Loss of one receptor, TlpD, came the closest to phenocopying the antral colonization defect observed in the Che$^-$ mutant (Fig. 5A). In contrast, mutants lacking the TlpA, TlpB, or TlpC chemoreceptor had only slight defects in antral localization (Fig. 5A). To confirm these results, we repeated the experiment and included the transition zone. In this independent infection, the corpus and antrum colonization of TlpD again came closest to phenocopying the Che$^-$ antral colonization defect (Fig. 5A). Additionally, we observed that the Che$^-$ and TlpD mutants had significant defects in colonizing the transition zone (Fig. 5B). These findings suggested that the TlpD chemoreceptor is needed for *H. pylori* to flourish in the antrum and transition zone. Interestingly, we also observed that the Δ*tlpD* mutant had a significant colonization defect in the corpus (Fig. 5A), which was not observed with any other chemoreceptor mutant and was more significant than the slight colonization defect of the Che$^-$ strain in this region (Fig. 5A). We wanted to rule out the possibility that the *tlpD* mutant has a colonization defect that is general and not specific to the antrum. We therefore determined each strain's corpus/antrum ratio. If the *tlpD* mutant had a general defect, we would expect its corpus/antrum ratio to match that of the wild type. This analysis instead found that the *tlpD* mutant ratio was like that of the Che$^-$ mutant and not like that of the wild type (Table 2). Therefore, TlpD appears to

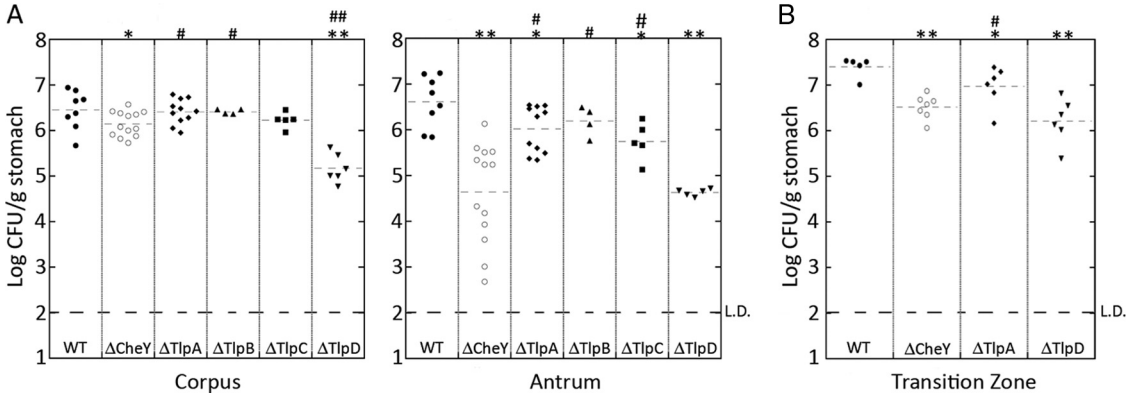

FIG 5 The chemoreceptor TlpD is necessary for antral colonization. FVB/N mice were infected with the wild type or a Che$^-$, TlpA$^-$, TlpB$^-$, TlpC$^-$, or TlpD$^-$ mutant for 2 weeks, at which time the stomachs were removed, divided into (A) the corpus and antrum or (B) the corpus, antrum, and C-A transition zone, and plated to enumerate *H. pylori* colonies. n = between 4 and 13. L.D., limit of detection. In comparison to the wild type, *, $P < 0.05$; **, $P < 0.0001$. In comparison to the Che$^-$ mutant, #, $P < 0.05$; ##, $P < 0.0001$ (Student's *t* test).

TABLE 2 Ratio of CFU/gram for the corpus versus the antrum[a]

Time PI and strain	Corpus/antrum ratio	
	Avg	Range
36 h		
WT	0.92	0.04–8.08
ΔCheY	1.05	0.29–18.0
2 wk		
WT	0.55	0.04–3.71
ΔCheY	12.0	2.08–1,117.74
ΔTlpA	1.90	0.57–15.62
ΔTlpB	1.39	0.75–4.96
ΔTlpC	2.30	1.75–6.76
ΔTlpD	5.19	1.10–507.35
6 mo		
WT	1.88	0.13–437.50
ΔCheY	8.96	3.32–2158.27

[a] Data are also presented in Fig. 3 to 5. PI, postinoculation.

be critical for specific *H. pylori* antral localization. Additionally, however, it seems that TlpD plays an important role in the corpus as well.

DISCUSSION

In this report, we provide evidence that bacterial chemotaxis promotes initial seeding in some stomach regions and the ability to rapidly multiply in others. Specifically, we found that *H. pylori* chemotaxis is needed to guide *H. pylori* to the corpus, but not to the antrum or transition zone, and that, once in the corpus, chemotaxis is not needed for *H. pylori* populations to increase. This finding suggests that nutrients are not limiting in the corpus, such that Che$^-$ mutants are able to obtain all that they need. The situation is different in the antrum and transition zone, where chemotaxis is required for the bacteria to achieve normal bacterial loads but not initial colonization. In these niches, Che$^-$ mutant numbers do not increase at the same rate as do those of the wild type. The main chemoreceptor that allows *H. pylori* to thrive in the antrum is TlpD, with the other chemoreceptors playing minor roles.

The mouse stomach has four distinct physiological regions: the forestomach, the corpus, the C-A transition zone, and the antrum (Fig. 1) (28). The gastric epithelium throughout the latter three regions is organized into repeating units called glands that invaginate from the surface. The glands in each stomach region are composed of different cells. The corpus glands contain zymogenic/digestive enzyme-secreting chief cells at the bottom and parietal/acid-producing cells, mucous neck cells, and mucous pit cells located progressively closer to luminal surface of the gland. There are also scattered but infrequent hormone-secreting enteroendocrine cells. The antrum similarly has scattered, infrequent enteroendocrine cells but, in contrast, has no parietal or chief cells. Instead, two types of mucous cells dominate these glands. One type is similar to the corpus mucous pit cells, while the other has properties that are a mixture of those of mucous neck cells and zymogenic cells (Fig. 1) (28, 36). Interestingly, mucin secreted by mucous neck cells inhibits *H. pylori* growth, while mucous pit cell mucin stimulates *H. pylori* growth (24). Accordingly, *H. pylori* has been found to occupy and replicate within the mucous pit cell mucin but not within the mucous neck cell mucin (23), suggesting that even within the distinctive stomach regions, there are some subareas more suitable for *H. pylori* than others.

The stomach regions described above present *H. pylori* with distinctive signals and challenges. For example, the cells in the antrum have a much higher turnover rate than those in the corpus, possibly increasing numbers of bacteria shed into the lumen (21). Also, mucous cells in both the corpus and the antrum secrete abundant superoxide anion (O_2-) (48); however, the corpus may temper the levels of these oxygen radicals with the high parietal cell expression of free radical scavengers (35). Parietal cells also secrete concentrated HCl, which presumably results in more frequent exposure to acid in the corpus. The pH of the corpus, however, is not lower overall than that of the antrum, although it does display a broader range (8, 32, 51). Thus, the different regions of the stomach possess distinct physiological characteristics that likely present *H. pylori* with different chemotactic signals.

H. pylori-induced disease depends of the localization of inflammation: gastritis in the antrum predisposes patients to duodenal ulcer, while gastritis in the corpus predisposes patients to gastric ulcers and cancer (3, 49). While it is unknown why inflammation develops in different stomach regions, one explanation could be that inflammation follows *H. pylori* density and that different *H. pylori* strains have distinct preferences for the corpus or the antrum (1). Three bacterial genetic determinants have been found that influence corpus-antrum distribution: the *cag*-PAI, the Fur transcription factor, and chemotaxis. Loss of *cagA* delivery, by mutation of either *cagA* or *cagY*, creates strains that do better in the gerbil antrum and worse in the corpus than their parents (40). These strains also induce reduced inflammation in both regions compared to the wild type. *H. pylori fur* mutants, in contrast, are found in nearly wild-type numbers in the antrum at 1 day postinoculation but decrease in antral numbers at day 3 postinoculation (33). These phenotypes suggest that *fur*, like chemotaxis, is not needed for antral seeding but is needed for replication. Also, like the Che$^-$ mutant defect, the *fur* defect is less significant in the corpus. Fur regulates some chemotaxis genes, such as *cheV1*, possibly explaining the overlapping phenotypes (13, 33). Thus, these three bacterial properties affect corpus-antrum localization in different ways and suggest that normal *H. pylori* variations might influence stomach region density.

Our studies presented here demonstrate that chemotaxis does not help *H. pylori* locate the antrum but does help it achieve normal bacterial numbers in this region. This finding suggests that some parameter of the antrum is particularly difficult for *H. pylori* and that chemotaxis helps to overcome this challenge. We report here that one potentially challenging condition is the elevated inflammation found in the antrum, which we could detect at 6 months of infection. We did not, however, detect a correlation between inflammation grade and bacterial numbers, as also seen by Williams et al. (54). We did note, however, that there was greater variation in *H. pylori* numbers at later time points postinfection (Fig. 4A) than at earlier ones (Fig. 2 and 3). This difference may be a reflection of individual variation in the adaptive immune response to *H. pylori*, whereas the innate response, which drives earlier numbers, does not display as much variation. We do not yet know if early inflammatory events specifically in the antrum render this area inhospitable for growth in the first part of infection, but this possibility is consistent with our data.

Based on this information, we envision two possibilities: (i)

chemotaxis allows *H. pylori* to locate a nutrient source necessary for growth and survival in the antrum or (ii) chemotaxis allows *H. pylori* to detect and avoid damaging compounds, such as those created by the immune response. Increased inflammation could amplify the necessity for chemotaxis in either situation, as inflammation is known to alter the nutrient status by chelating critical metals such as iron, zinc, and manganese (9, 25), and inflammation also increases production of reactive oxygen species (ROS) during the host's strong oxidative stress response (4). *H. pylori* appears to experience significant ROS exposure, as evidenced by the high cellular levels of enzymes such as SodB, catalase, AhpC, MdaB, and NapA (4, 22, 53).

To help us determine the nature of the chemotactic signal required for growth or survival in the antrum, we investigated which chemoreceptor was responsible for antral localization. Our studies determined that TlpA, TlpB, and TlpC each had only a moderate role in antral colonization. We were somewhat surprised that the acid-sensing TlpB did not play a more dominant role in antral localization, as one might have predicted that acid could repel *H. pylori* from the corpus to drive antral colonization (10). While pH gradients have been shown to impact the orientation of *H. pylori* in the mucus (43), our results suggest that pH sensing by TlpB does not contribute to *H. pylori* localization in the murine antrum. We do not know, however, if TlpB contributes to the initial seeding of the corpus.

TlpD appears to play the dominant role in the antral colonization of *H. pylori*, as well as in colonization in other regions. Interestingly, the *tlpD* mutant had a colonization defect in the corpus that was more severe than that seen with the completely nonchemotactic Che$^-$ mutant. Although we do not yet know why *tlpD* mutants experience such a corpus challenge, it is possible that the remaining chemoreceptors—TlpA, TlpB, and TlpC—attract *H. pylori* to an unsuitable niche, and normally, TlpD would act to at least partially repel the bacteria from a fatal interaction in this region.

TlpD is the only cytoplasmic chemoreceptor in *H. pylori* (44). Schweinitzer et al. demonstrated that TlpD senses cellular energy levels via the electron transport chain (44). Thus, TlpD may allow *H. pylori* to find optimal energy-generating conditions in the antrum and therefore promote colonization. One possibility is that increased antral inflammation alters the metabolically optimal area for *H. pylori* growth. For example, inflammation creates new respiratory electron acceptors in *Salmonella* infection through ROS-driven formation of tetrathionate from thiosulfate (55). In the case of *H. pylori*, it may be that inflammation limits the metabolically favorable region. Another possibility is that TlpD directs a repellent response to a deleterious component of the immune system, which allows *H. pylori* to escape and survive. This idea is consistent with our observed corpus phenotype in which *tlpD* mutants are even more defective than Che$^-$ mutants. One possible noxious compound is ROS. Our unpublished observations support the idea that wild-type *H. pylori* has a repellent response to ROS that is mediated by TlpD (Williams and Ottemann, personal communication).

In summary, we have shown that chemotaxis plays distinct roles in colonizing specific stomach regions, suggesting that there are subtle chemotactic cues that differ across this organ. Surprisingly, chemotaxis promotes initial seeding in some regions and growth in others. One of the four *H. pylori* chemoreceptors, TlpD, plays a dominant role in the growth phenotype. We hypothesize that antral success requires detection of a limited energy source or movement away from deleterious immune responses.

ACKNOWLEDGMENTS

We acknowledge Susan Williams and Marla Hill for experimental assistance.

The described project was supported by grant number AI050000 (to K.M.O.) from the National Institute of Allergy and Infectious Diseases (NIAID) at the National Institutes of Health.

This work is solely our responsibility and does not necessarily represent the official views of the NIH.

REFERENCES

1. **Akada JK.** 2003. *Helicobacter pylori* tissue tropism: mouse-colonizing strains can target different gastric niches. Microbiology **149**:1901–1909.
2. **Andermann TM, Chen Y-T, Ottemann KM.** 2002. Two predicted chemoreceptors of *Helicobacter pylori* promote stomach infection. Infect. Immun. **70**:5877–5881.
3. **Atherton JC.** 2006. The pathogenesis of *Helicobacter pylori*-induced gastro-duodenal diseases. Annu. Rev. Pathol. **1**:63–96.
4. **Baik S-C, Youn H-S, Chung M-H.** 1996. Increased oxidative DNA damage in *Helicobacter pylori*-infected human gastric mucosa. Cancer Res. **56**:1279–1282.
5. **Beier D, Spohn G, Rappuoli R, Scarlato V.** 1997. Identification and characterization of an operon of *Helicobacter pylori* that is involved in motility and stress adaptation. J. Bacteriol. **179**:4676–4683.
6. **Bijlsma JJE, et al.** 2002. The *Helicobacter pylori* homologue of the ferric uptake regulator is involved in acid resistance. Infect. Immun. **70**:606–611.
7. **Cerda O, Rivas A, Toledo H.** 2003. *Helicobacter pylori* strain ATCC700392 encodes a methyl-accepting chemotaxis receptor protein (MCP) for arginine and sodium bicarbonate. FEMS Microbiol. Lett. **224**:175–181.
8. **Cilluffo T, et al.** 1990. Reproducibility of ambulatory gastric pH recordings in the corpus and antrum. Effect of food, time, and electrode position. Scand. J. Gastroenterol. **25**:1076–1083.
9. **Corbin BD, et al.** 2008. Metal chelation and inhibition of bacterial growth in tissue abscesses. Science **319**:962–965.
10. **Croxen MA, Sisson G, Melano R, Hoffman PS.** 2006. The *Helicobacter pylori* chemotaxis receptor TlpB (HP0103) is required for pH taxis and for colonization of the gastric mucosa. J. Bacteriol. **188**:2656–2665.
11. **Eaton KA, Radin MJ, Krakowka S.** 1995. An animal model of gastric ulcer due to bacterial gastritis in mice. Vet. Pathol. **32**:489–497.
12. **Eaton KA, Danon SJ, Krakowka S, Weisbrode SE.** 2007. A reproducible scoring system for quantification of histologic lesions of inflammatory disease in mouse gastric epithelium. Comp. Med. **57**:57–65.
13. **Ernst FD, et al.** 2005. Transcriptional profiling of *Helicobacter pylori* Fur- and iron-regulated gene expression. Microbiology **151**:533–546.
14. **Ernst FD, et al.** 2005. Iron-responsive regulation of the *Helicobacter pylori* iron-cofactored superoxide dismutase SodB is mediated by Fur. J. Bacteriol. **187**:3687–3692.
15. **Foynes S, et al.** 2000. *Helicobacter pylori* possesses two CheY response regulators and a histidine kinase sensor, CheA, which are essential for chemotaxis and colonization of the gastric mucosa. Infect. Immun. **68**:2016–2023.
16. **Freter R, Brickner H, Botney M, Cleven D, Aranki A.** 1983. Mechanisms that control bacterial populations in continuous-flow culture models of mouse large intestinal flora. Infect. Immun. **39**:676–685.
17. **Freter R, Brickner H, Fekete J, Vickerman MM, Carey KE.** 1983. Survival and implantation of *Escherichia coli* in the intestinal tract. Infect. Immun. **39**:686–703.
18. **Freter R, Stauffer E, Cleven D, Holdeman L, Moore R.** 1983. Continuous-flow cultures as in vitro models of the ecology of large intestinal flora. Infect. Immun. **39**:666–675.
19. **Genta RM, Huberman RM, Graham DY.** 1994. The gastric cardia in *Helicobacter pylori* infection. Hum. Pathol. **25**:915–919.
20. **GoersSweeney E, et al.** 2012. Structure and proposed mechanism for the pH-sensing *Helicobacter pylori* chemoreceptor TlpB. Structure **20**:1177–1188.
21. **Hansen O, Pedersen T, Larsen J.** 1976. Cell proliferation kinetics in normal human gastric mucosa. Gastroenterology **70**:1051–1054.
22. **Harris A, et al.** 2003. Catalase (KatA) and KatA-associated protein

(KapA) are essential to persistent colonization in the *Helicobacter pylori* SS1 mouse model. Microbiology **149**:665–672.
23. **Hidaka E, et al.** 2001. *Helicobacter pylori* and two ultrastructurally distinct layers of gastric mucous cell mucins in the surface mucous gel layer. Gut **49**:474–480.
24. **Kawakubo M, et al.** 2004. Natural antibiotic function of a human gastric mucin against Helicobacter pylori infection. Science **305**:1003–1006.
25. **Kehl-Fie TE, Skaar EP.** 2010. Nutritional immunity beyond iron: a role for manganese and zinc. Curr. Opin. Chem. Biol. **14**:218–224.
26. **Kuipers EJ.** 1998. Review article: relationship between Helicobacter pylori, atrophic gastritis and gastric cancer. Aliment. Pharm. Ther. **12**(Suppl 1):25–36.
27. **Lee A, et al.** 1997. A standardized mouse model of Helicobacter pylori infection: introducing the Sydney strain. Gastroenterology **112**:1386–1397.
28. **Lee E, Trasler J, Dwivedi S, Leblond C.** 1982. Division of the mouse gastric mucosa into zymogenic and mucous regions on the basis of gland features. Am. J. Anat. **164**:187–207.
29. **Lertsethtakarn P, Ottemann KM, Hendrixson DR.** 2011. Motility and chemotaxis in Campylobacter and Helicobacter. Annu. Rev. Microbiol. **65**:389–410.
30. **Licht TR, Christensen BB, Krogfelt KA, Molin S.** 1999. Plasmid transfer in the animal intestine and other dynamic bacterial populations: the role of community structure and environment. Microbiology **145**:2615–2622.
31. **McGee DJ, et al.** 2005. Colonization and inflammation deficiencies in Mongolian gerbils infected by *Helicobacter pylori* chemotaxis mutants. Infect. Immun. **73**:1820–1827.
32. **McLauchlan G, Fullarton GM, Crean GP, McColl KE.** 1989. Comparison of gastric body and antral pH: a 24 hour ambulatory study in healthy volunteers. Gut **30**:573–578.
33. **Miles S, et al.** 2010. Detailed *in vivo* analysis of the role of *Helicobacter pylori* Fur in colonization and disease. Infect. Immun. **78**:3073–3082.
34. **Miller LD, Russell MH, Alexandre G.** 2009. Diversity in bacterial chemotactic responses and niche adaptation. Adv. Appl. Microbiol. **66**:53–75.
35. **Mills JC, et al.** 2001. A molecular profile of the mouse gastric parietal cell with and without exposure to *Helicobacter pylori.* Proc. Natl. Acad. Sci. U. S. A. **98**:13687–13692.
36. **Mills JC, Shivdasani RA.** 2011. Gastric epithelial stem cells. Gastroenterology **140**:412–424.
37. **Pittman MS, Goodwin M, Kelly DJ.** 2001. Chemotaxis in the human gastric pathogen Helicobacter pylori: different roles for CheW and the three CheV paralogues, and evidence for CheV2 phosphorylation. Microbiology **147**:2493–2504.
38. **Polk DB, Peek RM.** 2010. *Helicobacter pylori*: gastric cancer and beyond. Nat. Rev. Cancer **10**:403–414.
39. **Rader BA, et al.** 2011. *Helicobacter pylori* perceives the quorum-sensing molecule AI-2 as a chemorepellent via the chemoreceptor TlpB. Microbiology **157**:2445–2455.
40. **Rieder G, Merchant JL, Haas R.** 2005. Helicobacter pylori cag-type IV secretion system facilitates corpus colonization to induce precancerous conditions in Mongolian gerbils. Gastroenterology **128**:1229–1242.
41. **Rolig AS, Carter JE, Ottemann KM.** 2011. Bacterial chemotaxis modulates host cell apoptosis to establish a T-helper cell, type 17 (Th17)-dominant immune response in Helicobacter pylori infection. Proc. Natl. Acad. Sci. U. S. A. **108**:19749–19754.
42. **Rugge M, et al.** 2002. Gastric mucosal atrophy: interobserver consistency using new criteria for classification and grading. Aliment. Pharm. Ther. **16**:1249–1259.
43. **Schreiber S, et al.** 2004. The spatial orientation of *Helicobacter pylori* in the gastric mucus. Proc. Natl. Acad. Sci. U. S. A. **101**:5024–5029.
44. **Schweinitzer T, et al.** 2008. Functional characterization and mutagenesis of the proposed behavioral sensor TlpD of *Helicobacter pylori.* J. Bacteriol. **190**:3244–3255.
45. **Sipponen P, Hyvarinen H.** 1993. Role of *Helicobacter pylori* in the pathogenesis of gastritis, peptic ulcer and gastric cancer. Scand. J. Gastroenterol. Suppl. **196**:3–6.
46. **Symonds EL, Butler RN, Omari TI.** 2000. Assessment of gastric emptying in the mouse using the [13C]-octanoic acid breath test. Clin. Exp. Pharmacol. Physiol. **27**:671–675.
47. **Terry K, Williams SM, Connolly L, Ottemann KM.** 2005. Chemotaxis plays multiple roles during *Helicobacter pylori* animal infection. Infect. Immun. **73**:803–811.
48. **Teshima S, Rokutan K, Nikawa T, Kishi K.** 1998. Guinea pig gastric mucosal cells produce abundant superoxide anion through an NADPH oxidase-like system. Gastroenterology **115**:1186–1196.
49. **Uemura N, et al.** 2001. *Helicobacter pylori* infection and the development of gastric cancer. N. Engl. J. Med. **345**:784–789.
50. **van Vliet AH, et al.** 2002. The role of the ferric uptake regulator (Fur) in regulation of *Helicobacter pylori* iron uptake. Helicobacter **7**:237–244.
51. **Verdú EF, et al.** 1995. Effect of *Helicobacter pylori* status on intragastric pH during treatment with omeprazole. Gut **36**:539–543.
52. **Wadhams GH, Armitage JP.** 2004. Making sense of it all: bacterial chemotaxis. Nat. Rev. Mol. Cell Biol. **5**:1024–1037.
53. **Wang G, Alamuri P, Maier RJ.** 2006. The diverse antioxidant systems of Helicobacter pylori. Mol. Microbiol. **61**:847–860.
54. **Williams SM, et al.** 2007. Helicobacter pylori chemotaxis modulates inflammation and bacterium-gastric epithelium interactions in infected mice. Infect. Immun. **75**:3747–3757.
55. **Winter SE, et al.** 2010. Gut inflammation provides a respiratory electron acceptor for *Salmonella.* Nature **467**:426–429.
56. **Wroblewski LE, Peek RM, Wilson KT.** 2010. Helicobacter pylori and gastric cancer: factors that modulate disease risk. Clin. Microbiol. Rev. **23**:713–739.